

# Application of Response Surface Methodology and Artificial Neural Network in the Adsorption of Methylene Blue using Enhanced Chitosan Beads

Ephraim Igberase\*, Innocentia G. Mkhize

Department of Chemical Engineering, Durban University of Technology, Steve Biko, Durban, South Africa  
 ephraimi@dut.ac.za

A technique was developed to determine the adsorption of methylene blue (MB) from synthetic wastewater. On this note, chitosan beads (CS) were developed, the beads were cross-linked with glutaraldehyde (CCS) and thereafter grafted with aniline (GCCS). The properties of the developed materials were assessed utilizing XRD and BET. The study analyzed parameters, including pH, contact time, adsorbent dose, and initial concentration. These parameters were used as input data, while the output data was based on MB removal efficiency. For prediction and optimization, response surface methodology/central composite design (RSM-CCD) and artificial neural network (ANN) were applied for MB adsorption. Additionally, the relevance of these models was analyzed using statistical metrics. However, in developing the ANN model, 70% of the data was allocated for training, 15% for validation, and 15% for testing. Based on the RSM-CCD findings, the optimization outcome for the process parameters was obtained at a pH 7 adsorbent dose of 6 g, contact time of 55 min, and initial concentration of 125 mg/L. Consequently, an ideally trained neural network is described using training, testing, and validation phases, and the  $R^2$  values at these phases were found to be 1, 0.96837, and 0.96146, respectively. The statistical findings showed that the ANN approach outperforms the RSM model approach.

## 1. Introduction

Pollution emanating from cationic dyes in the environment causes many health problems. (Kang et al., 2021; Mokhtar et al., 2020; Wang et al., 2024). This cationic dye, including MB, can separate into positively charged ions in an aqueous solution. Industrial and agricultural practices are the most immediate reasons for this dye in wastewater. The food, paper, and leather industries are essential sources of highly industrialized wastewater (Ali et al., 2009). The release of MB into natural water bodies is destructive to natural creatures and ecosystems (Poshina et al., 2018). One such technology is adsorption, which has advantages such as low cost, environmentally friendly material for dye removal, and ease of use (Poshina et al., 2018). Many active adsorbents prepared from various materials, such as zeolites, chitosan, and many other materials, are used in MB removal (Mokhtar et al., 2020). Chitosan has an added advantage because of its bulky surface area, excellent adsorption, proper opening size, simple approachability, cost-effectiveness, mechanical stability, and environmental friendliness (Crini et al., 2019). The main goal of this work is to create a neural network model to predict the removal of MB from synthetic wastewater using a chitosan derivative as an adsorbent. With a design matrix from RSM-CCD, input and output data necessary to construct the technique and ANN models were gathered using a four-level design of experiments. The study takes a unique strategy in removing harmful dyes from wastewater by improving a natural adsorbent material and employing modern modeling tools. This innovative combination of material science and computational modeling shows great promise for producing practical and sustainable water treatment solutions.

## 2. Materials and methods

The experiment was carried out using high-quality chemicals, which included sodium hydroxide, acetic acid, hydrochloric acid, glutaraldehyde, and MB supplied by Sigma-Aldrich in South Africa. These chemicals had a

purity level of 99%. The pH of the mixture was adjusted using a benchtop pH meter. Distilled Water was obtained using an Ultima 888 water distiller. An incubator shaker was used for the adsorption experiments. During the formation of chitosan beads, 30g of chitosan powder was dissolved in 1 L of a 5.0% (v/v) acetic acid solution. A peristaltic pump passed the dissolved solution to a 1M sodium hydroxide solution via a glass pipette. Using a microwave oven, the resulting chitosan gel beads were cross-linked with glutaraldehyde and grafted with aniline. The Shimadzu XRD model 7000 equipment was used to study the crystalline nature of the developed materials. The sample's BET surface area, pore volume, and pore size were measured by nitrogen adsorption at 77 K using a Micromeritics (Australia) Tristar 3000 analyzer.

### 3. Results and discussion

#### 3.1 .XRD analysis

The crystallinity of the various developed materials\ was assessed through XRD. Foroutan et al. (2020) reported that chitosan is crystalline, and that the crystallinity blocks the amine group from adsorbing pollutants. Hence, modification is highly recommended to reduce the crystallinity of chitosan and open its network for easy diffusion of MB. The CS shown in Figure 1 exhibits a peak at  $2\theta = 20^\circ$ , Which corresponds to the 110 plane of chitosan. This same feature (110 plane) was also seen in CCS. This observation is because chitosan can retain some properties after a modification process. (Vieira et al., 2019). A decrease in intensity was observed when the cross-linked beads were grafted with aniline. The decreased intensity in the grafted sample caused the breaking of the original hydrogen bonds between amino and hydroxyl groups, thereby eliminating the crystallinity and creating a regular arrangement of polysaccharides. And thereby enhancing adsorption capacity.

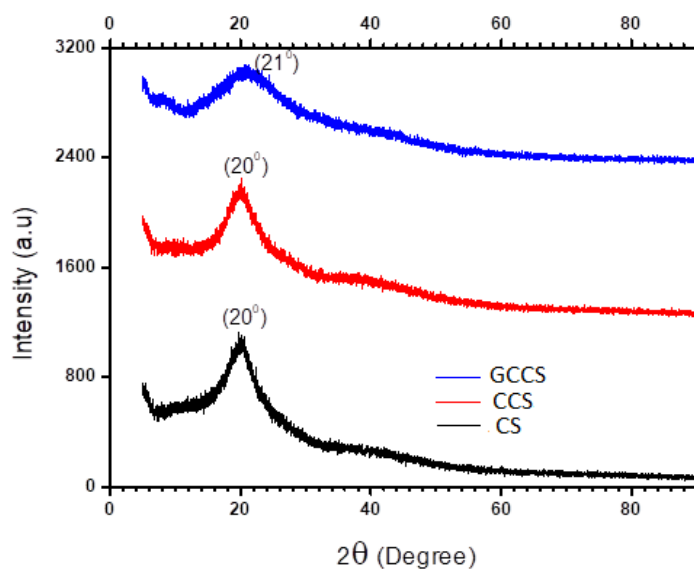


Figure 1: XRD for CS, CCS, and GCCS.

#### 3.2 BET result

Table 1 displays the BET surface area, pore volume, and pore size values for each set of beads. The surface area, pore volume, and pore size values of GCCS were substantially greater than those of other beads, as provided in the Table, which was helpful during adsorption. Additionally, the data demonstrated that cross-linking decreased pore diameters, pore volume, and surface area. This observation may be due to the chemical reaction between glutaraldehyde and chitosan, resulting in the loss of the amine group.

Table 1 BET surface area, pore volume, and pore size values of CS, CCS, and GCCS.

Sample	Surface area (m <sup>2</sup> /g)	Pore volume (cm <sup>3</sup> /g)	Pore size (nm)
CS	136.21	0.326	33.67
CCS	112.45	0.284	27.17
GCCS	208.32	0.402	42.15

### 3.3. RSM result

Design-Expert Version 6.0.6 was applied in the investigation. The model configuration of this study consisted of 21 experimental runs, with 16 of them as non-center points and five as center points, utilizing an alpha value of 1. The center points are essential because they offer a separate assessment of experimental error. Equation (1) presents an equation created by the model to explain quadratic polynomials. The RSM model was optimized by utilizing an objective function that varies from zero to one.

$$\gamma = \beta_0 + \sum_{i=1}^K \beta_i X_i + \sum_{i=1}^K \beta_{ii} X_i^2 + \sum_{i < j} \beta_{ij} X_i X_j + e(X_1, X_2, \dots, X_K) \quad (1)$$

The results obtained were analyzed using ANOVA from expert design software. The polynomial equation in terms of coded factors and manipulating one variable while keeping the others constant was used to fit the experimental design (Equation 2). The experimental and predicted values indicate that the design matrix was highly accurate. This is in accord with findings from (Sasidharan and Kumar, 2022), who reported that the higher.  $R^2$  Value signifies that the design matrix is well-fitted and reliable. Table 2 presents the experimental design/matrix and the related response for binding MB onto GCCS. This table illustrates how various parameters impact the outcome.

$$Y = +26.57 + 5.73A + 1.08B + 13.51C + 3.90D - 4.31A^2 - 2.14B^2 - 2.83C^2 - 1.38D^2 + 0.023AB + 5.60AC + 1.28AD - 0.15BC + 1.09BD + 1.99CD \quad (2)$$

$$R^2 = 0.9939$$

$$R^2_{adj} = 0.9854$$

Table 2: The layout of the model

STD	Factor 1 A: pH	Factor 2 B: Adsorbent dose (g)	Factor 3 C: Initial concentration (mg/L)	Factor 4 D: Contact time (Min)	Response: MB removal (%)
1	10.00	2.00	200.00	100.00	49.63
2	10.00	2.00	50.00	100.00	72.07
3	10.00	10.00	200.00	10.00	59.63
4	4.00	10.00	50.00	100.00	85.07
5	10.00	10.00	50.00	10.00	73.07
6	4.00	2.00	200.00	10.00	35.63
7	4.00	10.00	200.00	100.00	78.63
8	4.00	2.00	125.00	10.00	59.07
9	4.00	6.00	125.00	55.00	91.61
10	10.00	6.00	125.00	55.00	80.61
11	7.00	6.00	125.00	10.00	88.61
12	7.00	6.00	50.00	100.00	90.79
13	7.00	6.00	50.00	55.00	96.41
14	7.00	6.00	125.00	55.00	80.48
15	7.00	2.00	125.00	55.00	75.61
16	7.00	10.00	125.00	55.00	74.61
17	7.00	6.00	125.00	55.00	93.47
18	7.00	6.00	125.00	55.00	92.47
19	7.00	6.00	125.00	55.00	92.47
20	7.00	6.00	125.00	55.00	92.47
21	7.00	6.00	125.00	55.00	92.47

### 3.4 3D RSM plots

Figure 2 depicts the correlation between the two variables and their influence on the percentage removal of MB while holding other parameters constant. This plot demonstrates that the highest MB removal on GCCS occurs at pH 7, emphasizing the impact of pH on the adsorption process. According to the findings of (Mihaly Cozmuta et al., 2012), pH is essential in adsorption processes since it plays a significant role in the ionization of chemically reactive sites on the surface of the adsorbent. The effect of contact time on the binding of MB is also seen in this figure. The contact time was varied between 10 and 100 minutes, and it was proven that a contact time of 55 minutes was adequate for maximum removal of MB. This is due to the presence of well-aligned binding sites that are conveniently available for the adsorption of MB.

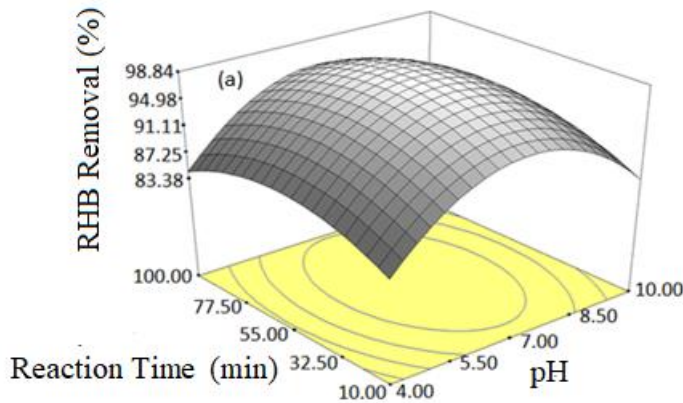


Figure 2: Effects of adsorbent dose and time

### 3.5 ANN result

This research applied the ANN technique with the help of the ANN Toolbox V4.0 in MATLAB 2019. Changing the network parameters altered the coding process conditions for Levenberg-Marquardt (LM). The LM could only make 10 data passes during data simulations. Also, no early stopping mechanism was used during the LM training. Figure 3 displays a well-established three-layer system with four neurons in the input layer, indicating contact time, solution pH, adsorbent dose, and concentration, which is used to model and forecast MB elimination. There are ten nodes in the hidden layer and one neuron in the output layer. Figure 4 shows how the network interacts with the training, testing, and validation data; correlation coefficients were found to be 0.95613, 1, 1, and 0.97017 for training, testing, validation, and overall data, respectively. The predicted results from the model correlate with the experimental data. The ANN model has great prediction ability, as shown by the overall correlation coefficient, and is suited for accurately predicting data.

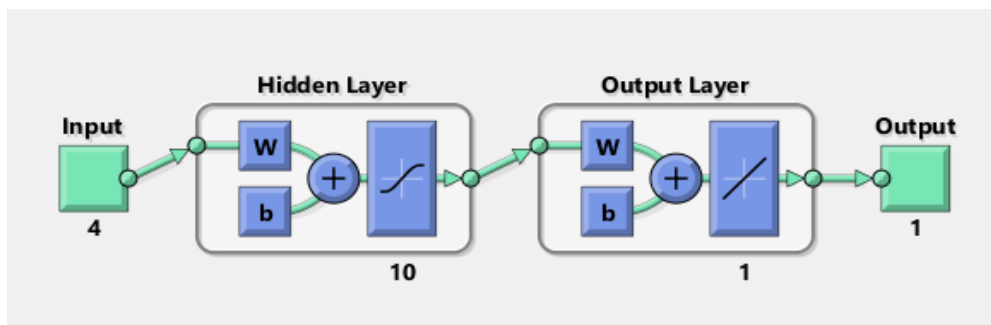


Figure.3: The ANN architecture

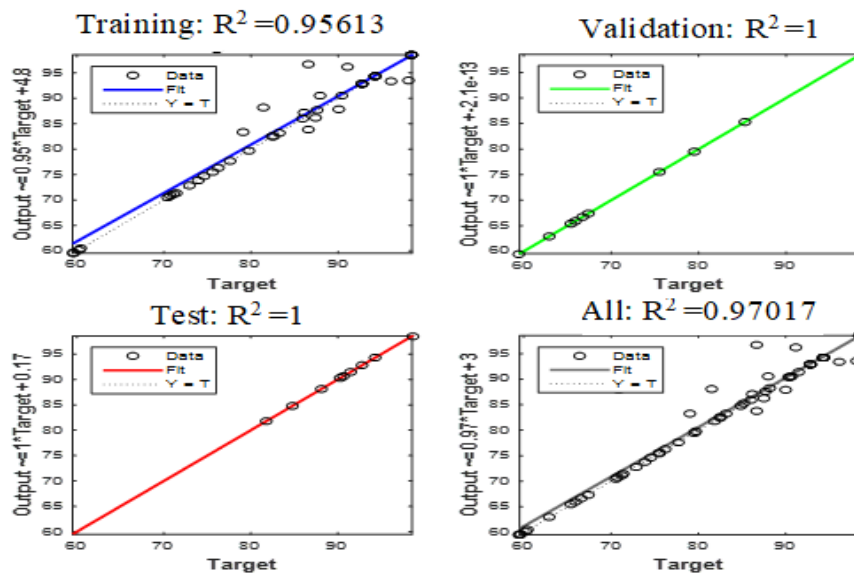


Figure 4: Regression plot for L-M model

In Table 3, one experiment was considered at the level of the process parameters. ANN and RSM models were assessed to predict MB removal efficiency. The comparison of actual and predicted removal efficiencies (%) showed that ANN and RSM models can predict values close to actual values. The statistical significance and error distribution of elimination efficiencies predicted by RSM and ANN were further assessed to compare the sufficiency of both models. In Table 4, the non-linear statistical metrics were applied to determine the size and measure error distribution for the RSM and ANN techniques. A reduced error function value was obtained for ANN when compared to RSM. The statistical metrics and prediction methods of the ANN model exceed those of the RSM model, which confirms the accuracy of the model.

Table 3: Comparison of the ANN and RSM-predicted and experimental values for the MB removal efficiency (input variables are  $pH=7.00$ , adsorbent dose = 6 g, contact time = 55.00 min, and initial concentration = 125.00 mg/L).

A	% removal Actual	% removal (ANN) Predicted	% removal (RSM) Predicted
Pb <sup>2+</sup>	98.44	98.47	98.52

Table 4: Non-linear error function fit for ANN and RSM.

Error function	ANN	RSM
Marquart's percent standard deviation (MPSD)	0.0001	0.0532
Chi-square test ( $\chi^2$ )	0.0017	0.0411
Root mean square error (RMSE)	0.0004	0.0732
Mean squared error (MSE)	0.0007	0.0011
The sum of the squares of errors (SSE)	0.0009	0.0031
Average relative errors (ARE)	0.0003	0.0320

### 3.6 Mechanism of adsorption

MB is a cationic dye with a positive charge in aqueous solutions, whereas GCCS has negatively charged functional groups, such as deprotonated groups, at specific pH values. These oppositely charged entities form a strong electrostatic attraction, the principal mechanism in neutral to slightly alkaline pH conditions. Also, MB has aromatic rings, allowing it to interact with functionalized chitosan through  $\pi$ - $\pi$  stacking. Depending on how the bead is modified, these interactions offer more binding. Improvements like grafting or cross-linking raise the porosity and surface area of the chitosan bead. It improves overall efficiency by ensuring more active sites are available for dye adsorption. At low pH, the protonation of the GCCS surface makes it positively charged and electrostatically repels MB. Functional groups are deprotonated at neutral or slightly alkaline pH, maximizing Electrostatic attraction via adsorption on the opposing surface charge. Adsorption may be stabilized or decreased at high pH values because of competition with OH ions. Hydrogen bonding and electrostatic interactions (the principal factors of MB adsorption onto GCCS) are mediated by van der Waals forces and  $\pi$ - $\pi$  interactions. The functional alterations of the beads and the expanded surface area ensure that the proposed beads will have high adsorption capacity and efficiency. This combination enables beads to perform the dual functions of dye adsorption and efficient cleaning solutions for eliminating MB from wastewater with reliability and environmental benefits.

### 4. Conclusion

Simulations employing RSM and ANN were used to assess the efficiency of MB removal from wastewater. The combination of RSM with ANN offers synergistic benefits to modeling and optimization techniques. RSM was conducted with CCD and annihilated with an ANN's LM training network. The accuracy of the removal efficiency prediction was compared using quality of fit ( $R^2$ ) analysis and error functions. The MB removal efficiency was accurately predicted with both models. The experimental result and the RSM/ANN predicted result are pretty effective. Results of RSM-CCD and ANN showed that modeling can reproduce and predict process behavior. Statistical analyses, as well as  $R^2$  values, are better with the ANN model. Equations for the MB model were established using collections of experimental data. The experimental findings and the predicted values were in excellent agreement.

### References

- Foroutan R, Peighambaroust S, Mohammadi R, Omidvar M, Sorial G, Ramavandi R, 2020. Influence of chitosan and magnetic iron nanoparticles on chromium adsorption behavior of natural clay: Adaptive neuro-fuzzy inference modeling. *Int J Biol Macromol* 151, 355–365.
- Kang, S. Bin, Wang, Z., Won, S.W., 2021. Evaluation of Adsorption and Desorption Properties of PAAPSBF for Cd(II) from Aqueous Solution. *Chem Eng Trans* 89, 259–264. <https://doi.org/10.3303/CET2189044>
- Mihaly Cozmuta, L., Mihaly Cozmuta, A., Peter, A., Nicula, C., Bakatula Nsimba, E., Tutu, H., 2012. The influence of pH on the adsorption of lead by Na-clinoptilolite: Kinetic and equilibrium studies. *Water SA* 38, 269–278. <https://doi.org/10.4314/wsa.v38i2.13>
- Mokhtar, A., Abdelkrim, S., Djelad, A., Sardi, A., Boukoussa, B., Sassi, M., Bengueddach, A., 2020. Adsorption behavior of cationic and anionic dyes on magadiite-chitosan composite beads. *Carbohydr Polym* 229. <https://doi.org/10.1016/j.carbpol.2019.115399>
- Sasidharan, R., Kumar, A., 2022. Response surface methodology for optimization of heavy metal removal by magnetic biosorbent made from anaerobic sludge. *Journal of the Indian Chemical Society* 99. <https://doi.org/10.1016/j.jics.2022.100638>
- Vieira, M.L.G., Pinheiro, C.P., Silva, K.A., Lutke, S.F., Cadaval, T.R.S.A., Dotto, G., Pinto, L.A. de A., 2019. Chitosan and cyanoguanidine-crosslinked chitosan coated glass beads and its application in fixed bed adsorption. *Chem Eng Commun* 206, 1485–1497. <https://doi.org/10.1080/00986445.2019.1581618>
- Wang, M., Yan, R., Shan, M., Liu, S., Tang, H., 2024. Fabrication of crown ether-containing copolymer porous membrane and their enhanced adsorption performance for cationic dyes: Experimental and DFT investigations. *Chemosphere* 352. <https://doi.org/10.1016/j.chemosphere.2024.141363>